Room-temperature mid-infrared “M”-type GaAsSb/InGaAs quantum well lasers on InP substrate

Chia-Hao Chang, Zong-Lin Li, Chien-Hung Pan, Hong-Ting Lu, Chien-Ping Lee, and Sheng-Di Lin

Citation: Journal of Applied Physics **115**, 063104 (2014); doi: 10.1063/1.4865170
View online: http://dx.doi.org/10.1063/1.4865170
View Table of Contents: http://scitation.aip.org/content/aip/journal/jap/115/6?ver=pdfcov
Published by the AIP Publishing

Room-temperature mid-infrared "M"-type GaAsSb/InGaAs quantum well lasers on InP substrate

Chia-Hao Chang, Zong-Lin Li, Chien-Hung Pan, Hong-Ting Lu, Chien-Ping Lee, and Sheng-Di Lin[a)]
Department of Electronics Engineering, National Chiao Tung University, 1001 University Road, Hsinchu 30010, Taiwan

(Received 16 January 2014; accepted 28 January 2014; published online 12 February 2014)

We have demonstrated experimentally the InP-based "M"-type GaAsSb/InGaAs quantum-well (QW) laser lasing at 2.41 μm at room temperature by optical pumping. The threshold power density per QW and extracted internal loss were about 234 W/cm^2 and 20.5 cm^{-1}, respectively. The temperature-dependent photoluminescence (PL) and lasing spectra revealed interesting characteristics for this type of lasers. Two distinct regions in the temperature dependent threshold behavior were observed and the transition temperature was found to coincide with the cross over point of the PL and lasing emission peaks. The current-voltage characteristic of "M"-type QW laser was superior to the inverse "W"-type one due to its thinner barrier for holes. Further improvement of the "M"-type QW structure could lead to a cost-effective mid-infrared light source. © *2014 AIP Publishing LLC*. [http://dx.doi.org/10.1063/1.4865170]

I. INTRODUCTION

Molecular absorption spectroscopy is an important tool to identify various gas molecules in chemical gas analysis and atmospheric pollution monitoring. Every molecule has its inherent absorption spectra. For example, there are strong absorption lines for NH_3 around 2.1 μm, for CO around 2.3 and 4.6 μm, for CH_4 around 2.35 and 3.3 μm, etc.[1] In this mid-infrared wavelength range of 2–5 μm, many different kinds of laser sources are available. But aiming for integrating with photodetectors to build a complete measurement system, the size of the laser has to be minimized. Semiconductor laser is an ideal choice for reaching a compact even portable system. In recent years, laser diodes operated in 2–3.5 μm wavelength range have been successfully demonstrated on GaSb substrates. By using the strained InGaAsSb quantum wells (QWs) as the active region, lasers with a low threshold current density (44 A/cm^2) were demonstrated.[2] On the other hand, mid-infrared lasers built on cost-effective InP substrates could be a better alternative because of its high thermal conductivity and mature fabrication technology, comparing with GaSb-based devices. However, there is no narrow bandgap material lattice-matched to InP to allow operation in such wavelength range. So Sato *et al*. used highly strained InAs QWs to extend the lasing wavelength and the longest lasing wavelength was 2.33 μm.[3] To achieve even longer wavelength, one can use structures with type-II band alignment where electrons and holes are confined in different spatial locations and the emission wavelength is not limited by the bandgap of the constituent materials. But the emission efficiency is usually not as good as those of type-I structures. Recently, "W"-type structures on InP and GaSb substrates were proposed to enhance the electron-hole wavefunction overlap as well as the radiative recombination in type-II band alignment.[4–10] In InP-based InGaAs/GaAsSb "W"-type structure, our previous theoretical study shows that, without serious degradation of the emission efficiency, the wavelength is tunable in the range of 2–3 μm by properly setting the composition and the width of InGaAs and GaAsSb layers.[11] The optically pumped "W"-type laser at 2.56 μm was realized at room temperature soon after.[12] However, a large turn-on voltage of the same structure with doped cladding layers was a serious problem for laser operation under electrical injection. This is largely due to the difficulty of hole transport in the multiple QWs region.

An inverse structure, denoted as "M"-type here, could be able to improve the problem of hole transport in "W"-type QWs as we shall discuss below. Such structure has been successfully used in infrared photodetectors.[13] Very recently, the "M"-type QW on InP substrate was proposed theoretically as a promising structure for mid-infrared light sources[14] but no corresponding experimental result has been reported. In the present work, we experimentally investigate the "M"-type GaAsSb/InGaAs/GaAsSb QWs with reduced hole barriers so the electrical transport property has been improved. The first lasing for "M"-type laser at 2.41 μm at room temperature is observed with optical pumping. Recently, by replacing InAlAs with GaAsSb layer to lower the barrier of electron and hole, the electrically driven "W"-type laser diodes were demonstrated with a high threshold current density of about 2 kA/cm^2.[15,16] We expect that, by using "M"-type QWs instead, the threshold current density could be lowered. The initial result on the I-V characteristics of the "M"-type structure showed superior turn-on behavior to that of "W"-type devices. We also analyzed the temperature-dependent lasing characteristics and the corresponding photoluminescence (PL). It revealed that the localized states played a key role to the abnormal phenomena of temperature-insensitive lasing wavelength.

[a)]Author to whom correspondence should be addressed. Electronic mail: sdlin@mail.nctu.edu.tw

II. SAMPLE GROWTH, DEVICE FABRICATION, AND MEASUREMENT METHODS

The sample was grown on S-doped (001) InP substrates by a Veeco GEN II solid-source molecular beam epitaxy (MBE) system. The As_2 and Sb_2 sources were supplied by the needle-valved cracker cells. Be and Si were used, respectively, as p- and n-typed dopants. The wafer surface temperature was monitored by an infrared pyrometer. To remove the native oxide on the surface, the substrate was de-oxidized under As_2 flux at 540 °C for 5 min. The growth started with a 100-nm-thick n-typed ($N_D = 1 \times 10^{18}\,cm^{-3}$) $In_{0.52}Al_{0.48}As$ layer and followed by a 200-nm-thick undoped $In_{0.52}Al_{0.48}As$ layer. The active region consisted of 15 periods of the "M"-type QWs (see Fig. 1). Every period had a symmetric $GaAs_{0.3}Sb_{0.7}/In_{0.53}Ga_{0.47}As/GaAs_{0.3}Sb_{0.7}$ (3/4/3 nm) well sandwiched between two $In_{0.36}Al_{0.32}Ga_{0.32}As$ (2 nm) barriers. The 5-nm spacing layers $In_{0.52}Al_{0.48}As$ were inserted to separate the "M"-type QWs. The active region was followed by a 160-nm-thick undoped $In_{0.52}Al_{0.48}As$ layer and a 2.1-μm-thick p-typed ($N_A = 1 \times 10^{18}\,cm^{-3}$) $In_{0.52}Al_{0.48}As$ layer. The growth was finished by 250-nm-thick p-typed ($N_A = 1 \times 10^{19}\,cm^{-3}$) $In_{0.53}Ga_{0.47}As$ contact layer. Regarding to the growth condition, the growth rates were 1.3 μm/h for $In_{0.36}Al_{0.32}Ga_{0.32}As$ layer, 0.9 μm/h for $In_{0.52}Al_{0.48}As$ and $In_{0.53}Ga_{0.47}As$ layers, and 0.4 μm/h for $GaAs_{0.3}Sb_{0.7}$ layer. The V/III beam equivalent pressure (BEP) ratios were 15 for $In_{0.36}Al_{0.32}Ga_{0.32}As$, $In_{0.52}Al_{0.48}As$, and $In_{0.53}Ga_{0.47}As$ layer and 20 for $GaAs_{0.3}Sb_{0.7}$ layer. The Sb_2/As_2 BEP ratio was about 2 for $GaAs_{0.3}Sb_{0.7}$ layer. The "M"-type region was grown at 470 °C but others were at 490 °C.

For PL measurements, the top $In_{0.53}Ga_{0.47}As$ and the p-typed $In_{0.52}Al_{0.48}As$ layers were removed by chemical etching to avoid the absorption of the excitation laser light, which was a 514.5 nm Ar-ion laser. The luminescence was dispersed through a monochromator and detected by a thermal-electric-cooled (TEC) InGaAsSb photodetector. The spectral response of the detector was calibrated by a black-body light source. For optical pumping experiment, the samples with the $In_{0.53}Ga_{0.47}As$ contact layer removed were excited by a 1064 nm (1.165 eV) pulsed fiber laser (pulse width: 10 ns, repetition rate: 1 kHz) with a beam diameter of around 1.3 mm. To define the pumping area, the gain guided laser devices with 100-μm-wide stripes were defined by openings in an evaporated gold metal mask. The lasers were two-side cleaved with four cavity lengths (800, 1000, 1100, and 1250 μm). In light-output vs. light-input (L-L) measurement, the laser emitted from the cleaved mirror was collimated by an aspheric lens and detected directly by a TEC InAs photodetector.

For the electrically driven laser devices, 20-μm wide ridge waveguide structures were fabricated by conventional photo-lithography and wet etching techniques. The metals for p- and n-typed ohmic contacts were Ti/Pt/Au and Ni/Ge/Au, respectively.

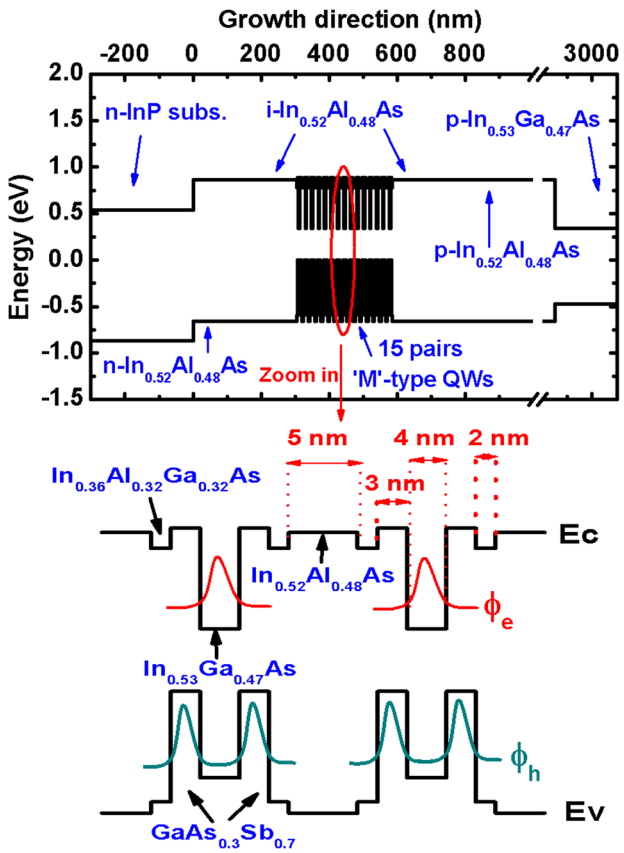

FIG. 1. Band diagram of the "M"-type laser sample. The zoom in part is two pairs of "M"-type QWs: $GaAs_{0.3}Sb_{0.7}$ is the hole well and $In_{0.53}Ga_{0.47}As$ is the electron well (thickness: $GaAs_{0.3}Sb_{0.7}/In_{0.53}Ga_{0.47}As/GaAs_{0.3}Sb_{0.7}$: 3/4/3 nm). $In_{0.52}Al_{0.48}As$ barrier layer is 5 nm; $In_{0.36}Al_{0.32}Ga_{0.32}As$ strain compensated layer is 2 nm.

III. RESULTS AND DISCUSSIONS

A. Temperature-dependent PL

The measured PL spectra taken at different temperatures were plotted in Fig. 2. Note that the spectra have been offset for clarity. At the lowest temperature (13 K), the PL peak was at 2300 nm with a full-width at half-maximum (FWHM) of 28.3 meV. As the temperature increased, from 13 to 99 K, the peak wavelength had a blue shift from 2300 to 2270 nm, which was in contrary to what one would expect from the bandgap shrinkage effect.[17] Similar phenomena had been observed in previous studies[18,19] and explained by the effect of localized states in the GaAsSb layer and/or at the InGaAs/GaAsSb interfaces. These localized states could be

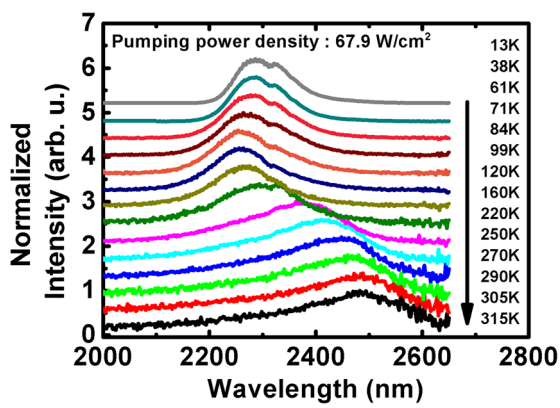

FIG. 2. Temperature dependent PL spectra from 13 K to 315 K. The excitation power density of Ar ion laser is 67.9 W/cm^2.

due to composition fluctuation, QW width fluctuation or interface roughness.[18–22] The energy levels of these states lay inside the bandgap, so the photo-generated carriers would be trapped at those levels at low temperatures and then radiatively recombined. With increasing temperature, the carriers occupied at the localized states would thermally escape to higher energy states thereby the emission peak shifted to the shorter wavelength. For the temperature higher than 99 K, the peak wavelength started to red shift due to bandgap shrinkage. In Fig. 3, we plotted the PL peak energy against temperature (the blue square symbol). The fitting curve (red line) using Varshni equation, $E_g(T) = E_0 - \alpha T^2/(T+\beta)$, was also plotted ($\alpha = 4.75 \times 10^{-4}$ eV/K, $\beta = 439.13$ K, $E_0 = 0.557$ eV). The fitting curve coincided with the experimental data very well for $T > 99$ K. However, at lower temperatures, a clear difference was seen. The difference at 13 K was about 18.4 meV. This energy had been defined as the localization energy of the localized states mentioned above.[18,19] In Fig. 3, we also showed the integrated PL intensity (the green open circles) as a function of temperature. Two distinct regions were clearly seen in this plot indicating the two different mechanisms mentioned above.

B. Optically pumped laser characteristics

The measured L-L curves of four lasers with different cavity lengths were shown in Fig. 4(a). The measured threshold power, P_{th}, was 13 W for the 1-mm long and 100-μm wide stripe at 295 K. By taking the surface reflection and QWs absorption into consideration, we estimated that only about 27% of the pumping light was absorbed by the active region. So the actual threshold power was about 3.51 W, which corresponded to a threshold power density of 234 W/cm^2 per QW. In the inset of Fig. 4(a), we showed the plot of the inverse quantum efficiency, $1/\eta_d$, versus cavity length (L). From the slope of the fitted line and the known facet reflectivity of 0.27, we obtained an internal loss (α_i) of about 20.5 cm^{-1} for the laser. The emission spectra of a laser with an 1-mm long and 100-μm wide cavity were shown below threshold ($0.86P_{th}$) and above threshold ($1.02P_{th}$) in Fig. 4(b). The dramatic increase of output power at threshold and the shrunk FWHM of the emission spectra were clear evidence of the lasing behavior. The lasing peak wavelength was 2414 nm at $1.02P_{th}$.

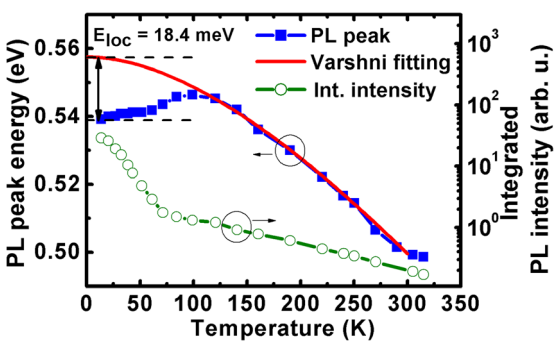

FIG. 3. Blue square symbols: PL peak energy at different temperature. Red line: the fitting curve by Varshni equation. E_{loc} is the energy difference between PL peak energy and the fitting energy at about 0 K (here is 13 K). Green open circle symbols: Integrated PL intensity at different temperature.

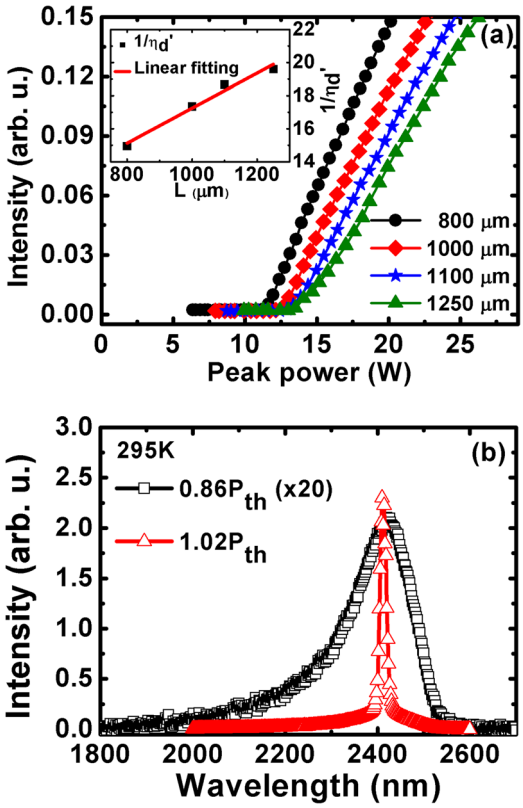

FIG. 4. (a) L-L curves of different cavity length (800, 1000, 1100, and 1250 μm) lasers at 295 K. The inset is the inverse of non-calibrated external quantum efficiency vs. cavity length. (b) Before threshold ($0.86P_{th}$, intensity $\times 20$) and after threshold ($1.02P_{th}$) spectra for 1 mm long and 100 μm wide laser at 295 K.

We also measured the threshold power density of a 1 mm long laser at different temperatures. The result, presented as a semi-log plot, was shown in Fig. 5(a). From 77 K to 250 K, the threshold power density increased slightly. By using $P_{th}(T) = P_{th0} \times \exp(T/T_0)$, we extracted a very high characteristic temperature T_0 of 862 K. After 250 K, the threshold power density rose rapidly and T_0 dropped to 47 K. Similar behaviors had been reported previously[12,23] and were explained by non-radiative Auger recombination near room temperature. However, we thought this sudden change in the temperature dependent behavior at 250 K could be from a different mechanism. If we carefully examined the PL spectra and the lasing spectra at different temperatures, we noticed that the peak positions of these two spectra were not the same and they cross each other at 250 K (see Fig. 5(b)). For $T < 250$ K, the lasing peak energy was lower than that of PL. With increasing temperature, the PL and lasing peak energies got closer to each other. This tended to reduce the threshold power for lasing and compensated the effect from the increased non-radiative recombination as the temperature rose. As a result, a nearly unchanged threshold power density was obtained for $T = 77$–250 K. When the temperature increased above 250 K, the PL peak energy dropped below the lasing peak. As the two peaks moved away from each other, the lasing threshold was increased. This, coupled with the temperature dependent non-radiative recombination, caused the characteristic temperature to go up suddenly at the cross over temperature. The nearly

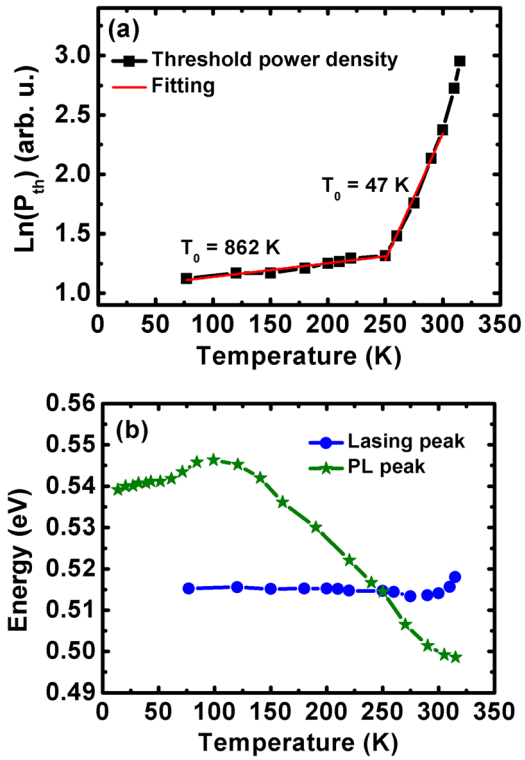

FIG. 5. (a) Black square symbols are the nature log of threshold power density versus temperature. Red lines are the fitting curves to extract characteristic temperatures. (b) Blue circle symbols are the lasing peak energy at threshold versus temperature. Green star symbols are the PL peak energy versus temperature.

constant lasing emission energy was most likely due to the competing effects from band-filling and bandgap shrinkage. The reason for the large difference in the emission energy between lasing and PL at low temperatures was not very clear. It could be caused by the heating from the large pumping power used for laser measurement. For $T > 300$ K, the lasing peak energy bent up due to the severe band-filling in the type-II heterostructure.[21]

C. I-V characteristic

The "M"-type sample was also fabricated into a ridge waveguide structure for electrical measurement. The devices had a length of 2 mm and a width of 20 μm. For comparison, a "W"-type laser with the same size was also fabricated. The only difference between the two was that the "M" structure used $GaAs_{0.3}Sb_{0.7}/In_{0.53}Ga_{0.47}As/GaAs_{0.3}Sb_{0.7}$ (3/4/3 nm) "M"-type QWs, while the "W" structure used the $In_{0.53}Ga_{0.47}As/GaAs_{0.3}Sb_{0.7}/In_{0.53}Ga_{0.47}As$ (4/3/4 nm) "W"-type QWs. Measured I-V curves of two devices were plotted in Fig. 6(a). For the "W"-type device, there were two turning points at about 2 and 4 V. The high turn-on voltage and two-step turn-on could be attributed to the difficult hole transport mentioned above.[15] The I-V curve of "M"-type laser was much better with normal turn-on characteristics. The reason for the superior I-V characteristics of the "M"-type devices could be seen in Fig. 6(b), which showed the comparison of the band diagrams of the two structures. In a "W"-type structure, the two electron wells were on the

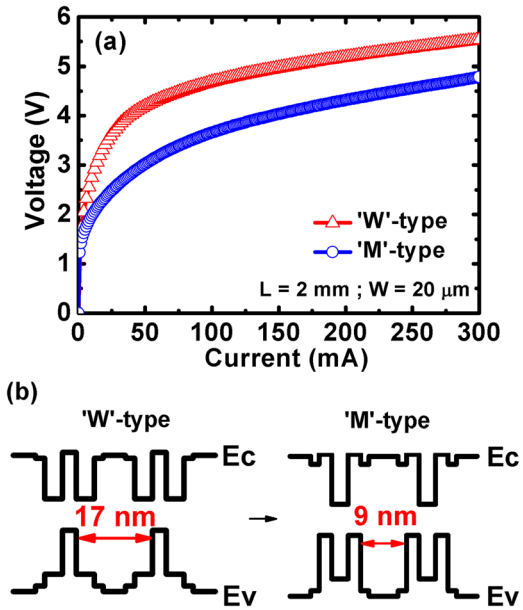

FIG. 6. (a) Blue empty circle symbols are the I-V curve of "M"-type diode. Red empty triangle symbols are the I-V curve of "W"-type diode. (b) The right side is the band diagram of "M"-type structure and the left side is the "W"-type structure. The hole barrier width is reduced from 17 nm to 9 nm by using "M"-type structure.

two sides of the middle hole well. When we stacked the "W" structures together, we could not put them too close to each other to avoid possible coupling between adjacent electron wells. But for the "M"-type structure, the hole wells were on the outside (or the center electron well). Because of a larger hole effective mass, we could stack the two "M" structures closer each other without worrying about the mutual coupling. For the two mirrored structures presented here, the "M" structure had a well spacing of 9 nm, but the "W" structure had 17 nm. The additional thickness caused the W structure to suffer from poor hole transport and worse turn on characteristics.

IV. CONCLUSION

We have presented the first room-temperature optically pumped "M"-type $GaAs_{0.3}Sb_{0.7}/In_{0.53}Ga_{0.47}As/GaAs_{0.3}Sb_{0.7}$ QWs laser lasing at 2.41 μm. The threshold power density per QW was 234 W/cm^2 and the extracted internal loss was 20.5 cm^{-1}. The characteristic temperature was about 862 K for temperatures between 77 K and 250 K but dropped to 47 K for temperatures above 250 K. By reducing the internal loss and further improving the carrier transport in the QW region, we believed a room-temperature, cost-effective, and electrically driven mid-infrared laser could be realized in the near future.

ACKNOWLEDGMENTS

We acknowledge the financial support from NSC and from ATU program of MOE in Taiwan. The equipment support from CNST and NFC at NCTU is appreciated.

[1]A. Joullié, P. Christol, A. N. Baranov, and A. Vicet, *Mid-Infrared 2–5 μm Heterojunction Laser Diodes* (Springer, 2003).
[2]K. K. Shirazi, K. Vizbaras, A. Bachmann, S. Arafin, and M. C. Amann, IEEE Photonics Technol. Lett. **21**, 1106 (2009).

[3]T. Sato, M. Mitsuhara, N. Nunoya, T. Fujisawa, K. Kasaya, F. Kano, and Y. Kondo, IEEE Photonics Technol. Lett. **20**, 1045 (2008).
[4]J. R. Meyer, C. A. Hoffman, and F. J. Bartoli, Appl. Phys. Lett. **67**, 757 (1995).
[5]S. Sprengel, C. Grasse, K. Vizbaras, T. Gruendl, and M. C. Amann, Appl. Phys. Lett. **99**, 221109 (2011).
[6]C. Grasse, P. Wiecha, T. Gruendl, S. Sprengel, R. Meyer *et al.*, Appl. Phys. Lett. **101**, 221107 (2012).
[7]C. L. Felix, W. W. Bewley, I. Vurgaftman, L. J. Olafsen, D. W. Stokes, J. R. Meyer, and M. J. Yang, Appl. Phys. Lett. **75**, 2876 (1999).
[8]W. W. Bewley, H. Lee, I. Vurgaftman, R. J. Menna, C. L. Felix, R. U. Martinelli, D. W. Stokes, D. Z. Garbuzov, J. R. Meyer, M. Maiorov, J. C. Connolly, A. R. Sugg, and G. H. Olsen, Appl. Phys. Lett. **76**, 256 (2000).
[9]C. L. Canedy, W. W. Bewley, J. R. Lindle, I. Vurgaftman, C. S. Kim, M. Kim, and J. R. Meyer, Appl. Phys. Lett. **86**, 211105 (2005).
[10]J. Hader, J. V. Moloney, S. W. Koch, I. Vurgaftman, and J. R. Meyer, Appl. Phys. Lett. **94**, 061106 (2009).
[11]C. H. Pan and C. P. Lee, J. Appl. Phys. **113**, 043112 (2013).
[12]C. H. Pan, C. H. Chang, and C. P. Lee, IEEE Photonics Technol. Lett. **24**, 1145 (2012).
[13]B. M. Nguyen and M. Razeghi, Proc. SPIE **6479**, 64790S (2007).
[14]B. Chen, A. L. Holmes, V. Khalfin, I. Kudryashov, and B. M. Onat, Proc. SPIE **8381**, 83810F (2012).
[15]S. Sprengel, A. Andrejew, K. Vizbaras, T. Gruendl, K. Geiger *et al.*, Appl. Phys. Lett. **100**, 041109 (2012).
[16]S. Sprengel, C. Grasse, P. Wiecha, A. Andrejew, T. Gruendl, G. Boehm, R. Meyer, and M. C. Amann, IEEE J. Sel. Top. Quantum Electron. **19**, 4 (2013).
[17]K. P. O'Donnell and X. Chen, Appl. Phys. Lett. **58**, 2924 (1991).
[18]G. Rainò, A. Salhi, V. Tasco, R. Intartaglia, R. Cingolani, Y. Rouillard, E. Tournié, and M. De Giorgi, Appl. Phys. Lett. **92**, 101931 (2008).
[19]M. Baranowski, M. Syperek, R. Kudrawiec, J. Misiewicz, J. A. Gupta, X. Wu, and R. Wang, Appl. Phys. Lett. **98**, 061910 (2011).
[20]A. At-Ouali, R. Y.-F. Yip, J. L. Brebner, and R. A. Masut, J. Appl. Phys. **83**, 3153 (1998).
[21]M. Dinu, J. E. Cunningham, F. Quochi, and J. Shah, J. Appl. Phys. **94**, 1506 (2003).
[22]W. Chen, B. Chen, J. Yuan, A. Holmes, and P. Fay, Appl. Phys. Lett. **101**, 052107 (2012).
[23]C. L. Felix, J. R. Meyer, I. Vurgaftman, C.-H. Lin, S. J. Murry, D. Zhang, and S.-S. Pei, IEEE Photonics Technol. Lett. **9**, 734 (1997).